Supplemental Appendix

Supplemental Materials and Methods

AAV

AAV-cTNT-Cre, AAV-cTNT-GFP and AAV-cTNT-GFP-version2 were described previously (1). *Actn2* coding sequences were synthesized (Integrated DNA technologies, gBlock) and cloned into AAV-cTNT-GFP-version2 to generate AAV-ACTN2^{WT}-GFP and AAV-ACTN2$^{\Delta E2\text{-}6}$-GFP plasmids. Full-length *Mrtfa* and dn*Mrtfa* sequences were amplified from cDNA (Dharmacon MMM1013-202859509) and cloned into AAV-cTNT-GFP-version2 to generate AAV-MRTFA-GFP and AAV-dnMRTFA-GFP plasmids.

AAV9 was prepared as previously described (1, 2). 140 µg AAV-ITR, 140 µg AAV9-Rep/Cap, and 320 µg pHelper (pAd-deltaF6, Penn Vector Core) plasmids were produced by maxiprep (Invitrogen, K210017) or Gigaprep (Invitrogen, K210009XP) and triple transfected into 10 15-cm plates of HEK293T cells using PEI transfection reagent (Polysciences, 23966-2). 60 h after transfection, cells were scraped off plates, resuspended in lysis buffer (20 mM Tris pH 8, 150 mM NaCl, 1 mM MgCl2, 50 µg/ml Benzonase) and lysed by three freeze-thaw cycles. AAV in cell culture medium was precipitated by PEG8000 (VWR, 97061-100), resuspended in lysis buffer and pooled with cell lysates. AAV was purified in a density gradient (Cosmo Bio USA, AXS-1114542) by ultracentrifugation (Beckman, XL-90) with a VTi-50 rotor and concentrated in PBS with 0.001% pluronic F68 (Invitrogen, 24040032) using a 100 kD filter tube (Fisher Scientific, UFC910024).

AAV titer was quantified by real-time PCR using a fragment of the TNT promoter DNA to make a standard curve. PCR primers for AAV quantification were 5'-TCGGGATAAAAGCAGTCTGG-3' and 5'-CCCAAGCTATTGTGTGGCCT-3'. SYBR Green master mix (Invitrogen, 4368577) was used in this quantification.

Echocardiography

Echocardiography was performed on a VisualSonics Vevo 2100 machine with Vevostrain software by an investigator blinded to genotype or treatment group. Animals were awake during this procedure and held in a standard handgrip.

In situ heart optical confocal sectioning

Hearts were dissected from euthanized animals and cannulated on a Langendorff apparatus. Hearts were perfused with perfusion buffer [10 mM Hepes (pH 7.4), 120.4 mM NaCl, 14.7 mM KCl, 0.6 mM KH_2PO_4, 0.6 mM Na_2HPO_4, 1.2 mM $MgSO_4$, 4.6 mM $NaHCO_3$, 30 mM Taurine, 10 mM 2,3-butanedione monoxime, 5.5 mM glucose] at room temperature for 10 min. Where indicated, FM 4-64 (Invitrogen, 13320), TMRM (source), or Hoechst 33342 (Invitrogen) dyes were added to the perfusion buffer at 2 µg/ml, 2 nM, and 4 µg/ml, respectively. After labeling, the heart was removed from the perfusion system, positioned on a glass-bottom dish, and immediately imaged using an inverted confocal microscope (Olympus FV3000RS).

Histological analysis

After the animals were euthanized by CO_2, hearts were harvested immediately and fixed by 4% paraformaldehyde overnight at 4 °C. Fixed hearts were cryoprotected by soaking in 15% sucrose followed by 30% sucrose at 4 °C. Hearts were embedded in tissue freezing medium (General Data, TFM-5). 10 μm cryo-sections were cut using a cryostat (Thermo Scientific, Microm HM 550).

Fast green and sirius red staining was performed on frozen sections. Sections were first washed with PBS for 5 min, fixed with pre-warmed Bouin's solution (Sigma, HT10132) at 55 °C for 1h and washed in running water. The sections were then stained with 0.1% Fast green (Millipore, 1040220025) for 10 min, washed with 1% acetic acid for 2 minutes, and rinsed with running water for 1 min. The sections were then stained with 0.1% sirius red (Sigma, 365548) for 30 min and washed with running water for 1 minute. The slides were treated with 95% ethanol once for 5 min, twice with 100% ethanol for 5min, and twice in Xylene for 5 min before being mounted with Permount (Fisher Scientific, SP15-500). Bright-field images of stained tissue sections were taken with a BZ-X700 all-in-one microscope (Keyence).

Cardiomyocyte isolation

Cardiomyocytes were isolated by retrograde collagenase perfusion. In brief, heparin-injected mice were anesthetized in an isoflurane chamber. Hearts were isolated and cannulated onto a Langendorff perfusion apparatus. 37 °C perfusion buffer was first pumped into the heart to flush out blood and equilibrate the heart. Collagenase II (Worthington, LS004177) was next perfused into the heart for 10 min at 37 °C to dissociate cardiomyocytes. The apex was cut from the digested heart, gently dissociated into single cardiomyocytes in 10% FBS/perfusion buffer and filtered through a 100 μm cell strainer to remove undigested tissues.

Flow Cytometry

Isolated cardiomyocytes were filtered with a 100 μm cell strainer, pelleted by centrifugation at 20 x g for 5 min and resuspended in ~1 ml cold perfusion buffer. FACS was performed using a BD AriaII SORP cell sorter with a 100 μm nozzle.

Contractility measurement

Calcium was re-introduced into isolated cardiomyocytes by treating cells with a series of 5 ml perfusion buffers containing 60 nM, 400 nM, 900 nM, and 1.2 μM $CaCl_2$. At each step, cardiomyocytes were allowed to sediment for 5 min at room temperature before cells being transferred to the next buffer with higher calcium concentration.

For the contractility assay, cardiomyocytes were plated on laminin-coated coverslips in MEM media with 10 mM 2,3-butanedione monoxime and incubated for 30 min at 37 °C and 5% CO_2. The coverslips were then transferred into a 37 °C flow chamber with 1.2 μM $CaCl_2$ perfusion buffer without BDM. FP- and FP+ cells were identified by epifluorescence imaging. Cardiomyocytes were electrically stimulated at 1 Hz and cell contraction was measured using an IonOptix system and a 40X objective. Contractile and non-contractile CMs were identified visually.

Fluorescence imaging and analysis

Immunofluorescent labeling was performed as described (2–4). Cardiomyocytes were fixed with 4% paraformaldehyde for 10~20 min, permeabilized by 0.1% Triton-100/PBS for 10 min and blocked in 4% BSA/PBS (blocking buffer) at 4°C overnight. Then the cells were incubated with primary antibodies diluted in blocking buffer overnight at 4 °C. After washes with blocking buffer, the cells were incubated with secondary antibodies and dyes at room temperature for 2 h. The cells were next washed with PBS and mounted with ProLong Diamond antifade mountant (Invitrogen, 36961) before imaging. All antibodies and dyes are listed in the Table S2.

Confocal fluorescent images were taken using Olympus FV3000RS inverted laser scanning confocal microscope with a 60X/1.3 silicone-oil objective. Fluorescence intensity was measured using ImageJ. AutoTT (5) was used to quantify T-tubule and sarcomere organization. Cell size and shape were manually measured on maximally projected images.

Electron microscopy analysis after fluorescence-activated cell sorting (FACS-EM)

Isolated cardiomyocytes in suspension were fixed with 4% paraformaldehyde for 30 min at room temperature. The fixed cells were next filtered by passing through a 100 μm cell strainer, pelleted by centrifugation at 20 x g for 5 min at room temperature and resuspended in ~1 ml perfusion buffer. FACS was performed as described above. After FACS, the cells were fixed again in a mixture of 2% formaldehyde and 2.5% glutaraldehyde in 0.1 M Sodium Cacodylate buffer, pH 7.4 overnight at 4°C. The cell pellets were next processed through a routine TEM protocol at the Harvard Medical School EM core. Images were taken using a JEOL 1200EX - 80kV electron microscope. Because of the size and stiffness of cardiomyocytes, fixed adult cardiomyocytes clog the FACS machine. As a result, FACS-EM currently only works for cardiomyocytes from P30 or younger mice.

RNA extraction and analysis

For RT-qPCR analysis using heart tissue, total RNA was purified using PureLink RNA Mini kit (Ambion, 12183025). Genomic DNA removal and reverse transcription was performed using the QuantiTech reverse transcription kit (Qiagen, 205311). Real-time PCR was performed using an ABI 7500 thermocycler.

For RT-qPCR using FACS sorted cells, FACS was performed as described above. Samples were collected in a cooling device. Immediately after FACS, cells were centrifuged at 13,000 rpm at 4°C to remove supernatant. Total RNA was purified using PureLink RNA Micro kit (Thermo Fisher, 12183016) and genomic DNA was removed by on-column DNase I digestion. Reverse transcription was performed using the SMART-Seq v4 Ultra Low Input RNA Kit (Clontech), which pre-amplified full-length cDNA before qPCR. Real-time PCR was performed using an ABI 7500 thermocycler.

RT-qPCR was performed using either SYBR Green or Taqman probes. For SYBR detection, *Nppa* detection primers were 5'-TTCCTCGTCTTGGCCTTTTG-3' and 5'-CCTCATCTTCTACCGGCATC-3'. *Nppb* detection primers were 5'-GTCCAGCAGAGACCTCAAAA-3' and 5'-AGGCAGAGTCAGAAACTGGA-3'. *mCherry* detection primers were 5'-ACGGCCACGAGTTTGAGATT-3' and 5'-CAAGTAGTCGGGGATGTCGG-3'. *Gapdh* (internal control) detection primers were 5'-AGGTCGGTGTGAACGGATTTG-3' and 5'-TGTAGACCATGTAGTTGAGGTCA-3'. For

Taqman quantification, *Actn2 and Gapdh* were also measured using Mm00473657_m1 (Invitrogen, 4453320) and mouse GAPD endogenous control (Invitrogen, 4352339E) assays, respectively.

RT-PCR detection of *Actn2* splicing variants was performed using GoTaq PCR master mix (Promega) and primers: 5'-CCATCCATCCATCCATTTCTC-3' and 5'-TCTTCCATCAGCCTCTCATTC-3'.

RNA-seq and data analysis

10 ng total RNA from FACS-isolated cardiomyocytes was reverse transcribed and full-length cDNA was specifically amplified by 8 PCR cycles using SMART-Seq v4 Ultra Low Input RNA Kit (Clontech) (6). RNA-seq libraries were constructed using Illumina's Nextera XT kit and single-end sequence reads were obtained using an Illumina NextSeq 500 sequencer.

RNA-seq reads were aligned to mm10 by STAR (7) and reads counts were calculated by FeatureCounts (8). DESeq2 was used to perform statistical analysis of differential gene expression (9). An adjusted P value of 0.05 was used as the cutoff to identify differentially regulated genes. GO term analysis was performed using GSEA analysis with ranked gene lists (10). To visualize read distribution on genomic loci, bigwig files, generated by deeptools (11) with normalized read count, were loaded into the Integrative Genomics Viewer (12).

AAV reporter assay

We defined the Tpm1 promoter as a genomic region from -715 bp to +81bp relative to the transcription start site of Tpm1 transcript variant 1. Both Tpm1 promoter and Loxp-Stop-Loxp sites were amplified using the *Rosa*^{Cas9GFP} mouse genome as templates, and next inserted into an AAV-mCherry plasmid. The full sequence of this reporter will be available upon request.

In the reporter assay, high-dose AAV reporter and low-dose AAV-Cre were mixed and injected into P1-P3 littermates that were either *Srf*$^{F/F}$*;Rosa*^{Cas9GFP} *or* *Srf*$^{F/F}$*;Rosa*^{Cas9GFP}genotypes. The hearts were collected at P14 for fluorescence imaging followed by real-time quantitative PCR of *mCherry* and *Gapdh.*

Western blot analysis

Heart tissues were homogenized in RIPA buffer (25 mM Tris pH7.4, 150 mM NaCl, 1% Triton X-100, 0.5% Na Deoxycholate, 0.1% SDS) buffer supplemented with protease inhibitor cocktail and Micrococcal Nuclease at ~33.3 mg/ml concentration. Heart lysates were denatured in 2X SDS sample buffer at 70 °C for 10 min, separated on a 4%-12% gradient gel (Invitrogen, Bolt gels, NW04122BOX), transferred to a PDVF membrane, and blocked by 4% milk/TBST. Primary antibodies were incubated with the membrane overnight at 4°C, followed by four 15 min TBST washes. HRP-conjugated secondary antibodies were probed for 1~2h at RT, followed by four 15 min TBST washes. After adding Immobilon Western chemiluminescent HRP substrate (Millipore, WBKLS0500), chemiluminescence was detected using a Li-Cor C-DiGit blot scanner. Antibodies used in this study are listed in Table S2.

Actin pelleting analysis

Actin pelleting experiments were performed using the G-Actin/F-actin In Vivo Assay Biochem Kit (Cytoskeleton, Inc.) with modifications. In brief, heart tissues were homogenized in tissue lysis and actin stabilizing buffer (50 mM PIPES pH 6.9, 50 mM KCl, 5 mM $MgCl_2$, 5 mM EGTA, 5% glycerol, 0.1% NP40, 0.1% Triton X-100, 0.1% Tween 20, 0.1% beta-mercaptoethanol) supplemented with ATP and protease inhibitors at 33 mg/ml concentration. The heart lysate was next incubated at 37 °C for 1 hr and centrifuged with a SW55Ti rotor for 1 hr at 33000 rpm at 20 °C. The pellet was dissolved in 8M Urea. The supernatant and pellets were diluted to the same volume in SDS sample buffer before Western Blot analysis.

As a positive control for actin pelleting, 1 μM Swinholide A was added into heart lysates before 37 °C incubation. Vehicle (ethanol) treatment was used as a control for Swinholide A treatment.

Subcellular fractionation of heart tissue

Cytoplasmic and nuclear fractions of heart tissues were generated using the Subcellular Protein Fractionation Kit for Tissues (Life Technologies # 87790) with modifications. In brief, heart tissues were homogenized in 350 μl cytoplasm extract buffer, and spun at 3000g at 4 °C for 5 min. The supernatant was treated as the cytoplasmic fraction. The pellet was resuspended and partially dissolved in 230 μl membrane extract buffer at 4 °C for 5 min. The lysate was next centrifuged at 3000g for 5 min. The pellet was resuspended in 90 μl nucleus extract buffer with micrococcal nuclease and dissolved at room temperature for 20 min. This mixture was next spun at 12000g for 5 min. The resulting supernatant was the nuclear fraction.

Co-immunoprecipitation

pFLAG-MRTFA-wt (Addgene #11978) and pFLAG-MRTFA-ΔN (Addgene #27176) were kind gifts from Ron Prywes (13). HA-tagged ACTC1-R64D cDNA was synthesized by Integrated DNA Technologies to replace FLAG-MRTFA to generate the pHA-ACTC1-R64D plasmid. Control plasmid is pCAG-Cas9 (Addgene #51142). These plasmids were transfected into HEK293T cells using polyethylenimine transfection reagents. The transfected cells were cultured for 48 h before being harvested in lysis buffer (10 mM Tris-HCl pH 7.5, 150 mM NaCl, 1 mM EDTA, 1% Triton-X100, protease/phosphatase inhibitor cocktail). HA- or FLAG- tagged proteins were pulled down using Anti-HA Magnetic Beads (Life Technologies # 88836) or Anti-FLAG® M2 Magnetic Beads (Sigma Aldrich # M8823-1ML), respectively. The beads were washed 3 times in lysis buffer, boiled, and probed for HA and FLAG expression by western blotting.

NIH3T3 culture and experiments

NIH3T3 cells were purchased from ATCC and cultured in DMEM+10%FBS+pen/strep medium. pFLAG-MRTFA-wt or pFLAG-MRTFA-ΔN plasmids were co-transfected with the pHA-ACTC1-R64D plasmid using polyethylenimine transfection reagents. Two days after transfection, the cells were collected for immunofluorescence of HA and FLAG tag.

References for Supplemental Methods

1. Y. Guo, *et al.*, Hierarchical and stage-specific regulation of murine cardiomyocyte maturation by serum response factor. *Nat. Commun.* **9**, 3837 (2018).
2. Y. Guo, *et al.*, Analysis of Cardiac Myocyte Maturation Using CASAAV, a Platform for Rapid Dissection of Cardiac Myocyte Gene Function In Vivo. *Circ. Res.* **120**, 1874–1888 (2017).
3. Y. Guo, Y. Kim, T. Shimi, R. D. Goldman, Y. Zheng, Concentration-dependent lamin assembly and its roles in the localization of other nuclear proteins. *Mol. Biol. Cell* **25**, 1287–1297 (2014).
4. Y. Guo, Y. Zheng, Lamins position the nuclear pores and centrosomes by modulating dynein. *Mol. Biol. Cell* **26**, 3379–3389 (2015).
5. A. Guo, L.-S. Song, AutoTT: automated detection and analysis of T-tubule architecture in cardiomyocytes. *Biophys. J.* **106**, 2729–2736 (2014).
6. S. Picelli, *et al.*, Smart-seq2 for sensitive full-length transcriptome profiling in single cells. *Nat. Methods* **10**, 1096–1098 (2013).
7. A. Dobin, *et al.*, STAR: ultrafast universal RNA-seq aligner. *Bioinformatics* **29**, 15–21 (2013).
8. Y. Liao, G. K. Smyth, W. Shi, featureCounts: an efficient general purpose program for assigning sequence reads to genomic features. *Bioinformatics* **30**, 923–930 (2014).
9. M. I. Love, W. Huber, S. Anders, Moderated estimation of fold change and dispersion for RNA-seq data with DESeq2. *Genome Biol.* **15**, 550 (2014).
10. A. Subramanian, *et al.*, Gene set enrichment analysis: a knowledge-based approach for interpreting genome-wide expression profiles. *Proc. Natl. Acad. Sci. U. S. A.* **102**, 15545–15550 (2005).
11. F. Ramírez, *et al.*, deepTools2: a next generation web server for deep-sequencing data analysis. *Nucleic Acids Res.* **44**, W160-5 (2016).
12. J. T. Robinson, *et al.*, Integrative genomics viewer. *Nat. Biotechnol.* **29**, 24–26 (2011).
13. B. Cen, *et al.*, Megakaryoblastic leukemia 1, a potent transcriptional coactivator for serum response factor (SRF), is required for serum induction of SRF target genes. *Mol. Cell. Biol.* **23**, 6597–6608 (2003).

Figure S1

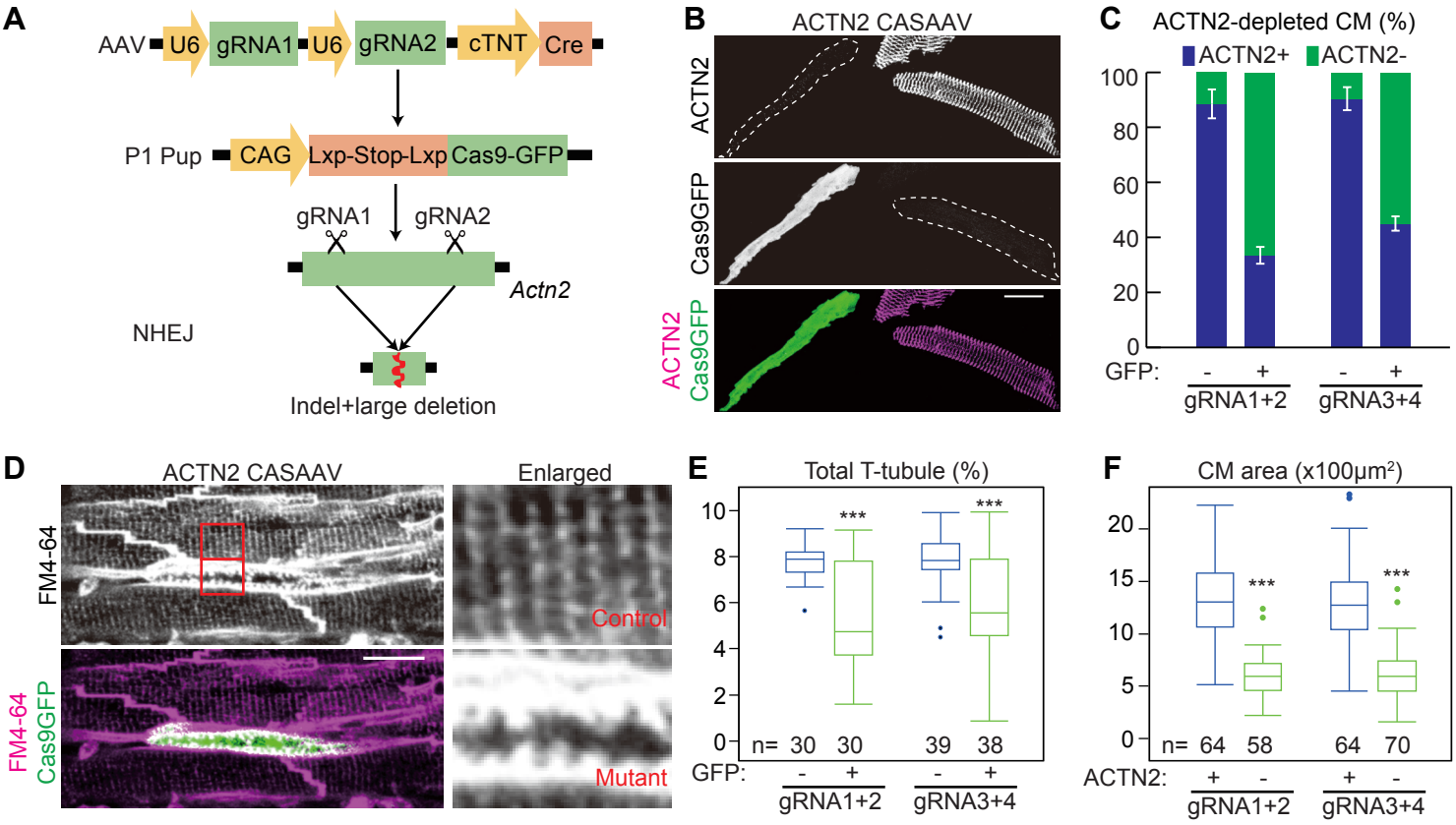

Fig. S1. CASAAV-based mutagenesis of *Actn2* causes morphological defects in CM maturation. (A) CASAAV-mediated somatic mutagenesis. AAV9 drives expression of two gene-targeting guide RNAs and cardiomyocyte-specific expression of Cre. Cre activates expression of Cas9 and GFP from the Rosa26 locus. The gRNAs direct Cas9 to cleave the target gene, e.g. *Actn2*, at one or both gRNA-targeted sites, and introduce loss-of-function mutations. **(B-C)** Efficiency of ACTN2 depletion by CASAAV. AAV was injected at P1. CMs were dissociated at P30 and immunostained for ACTN2 (B). Cell boundaries are delineated by white dashed lines. ACTN2 depletion in CASAAV-treated CMs (GFP+) was quantified (C). n=3 hearts per group; error bar, SD. **(D-E)** Effect of ACTN2 depletion on T-tubule morphology was analyzed by in situ imaging. CASAAV-treated P30 hearts were perfused with FM4-64, which labels the sarcolemma, and optically sectioned by confocal microscopy (D). Areas in red boxed are enlarged to the right. T-tubule content of GFP+ and GFP- cells was quantified using AutoTT (E). **(F)** Effect of ACTN2 depletion on CM size. Projected area of P30 dissociated CMs was plotted for cells with and without ACTN2 immunoreactivity. Student's t-test: ***p<0.001. Scale bars in (B) and (D) are 20 μm.

Figure S2

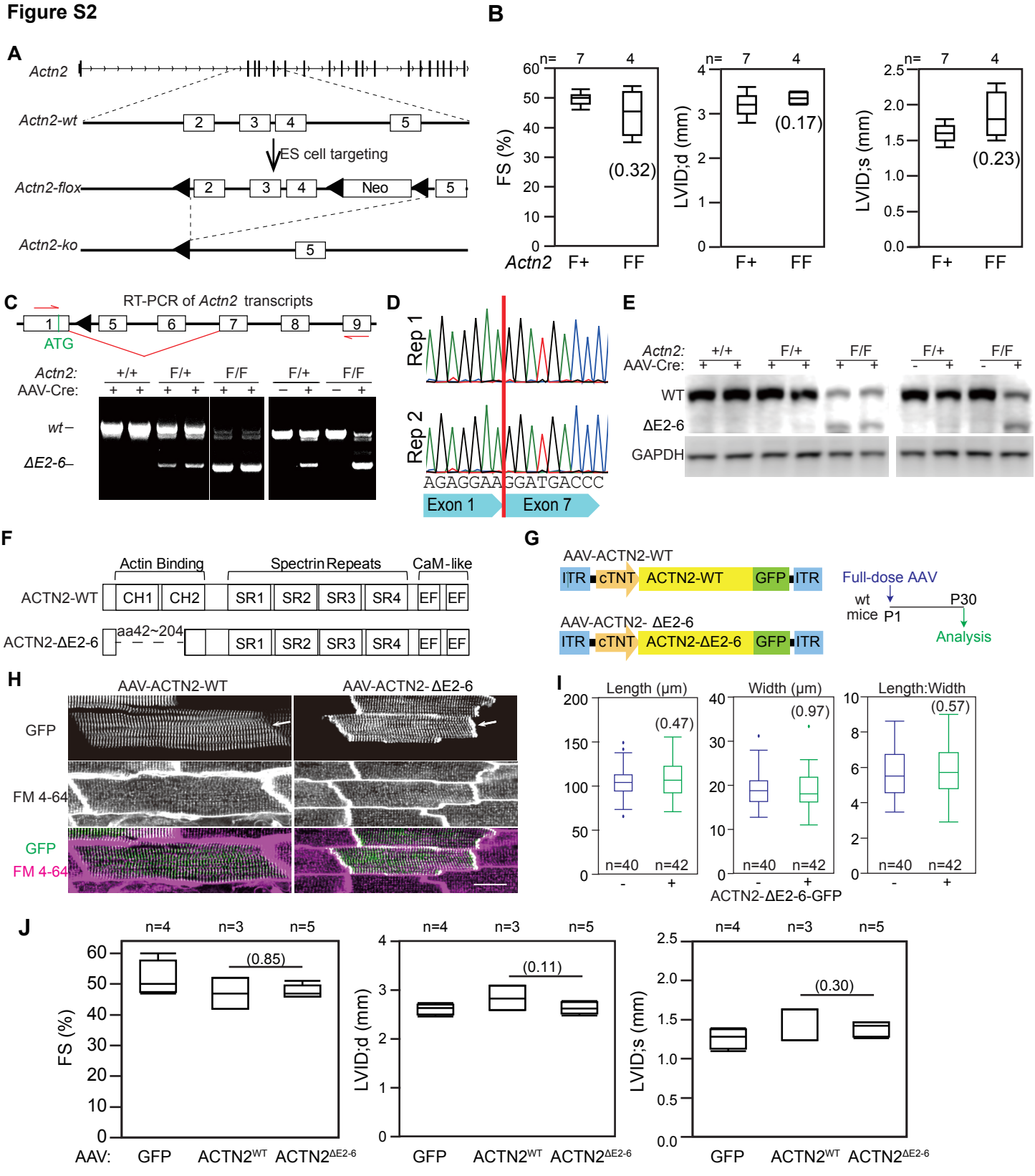
A
Actn2
Actn2-wt
2
3
4
5
ES cell targeting
Actn2-flox
Neo
Actn2-ko
B
n= 7 4
FS (%)
(0.32)
LVID;d (mm)
(0.17)
LVID;s (mm)
(0.23)
Actn2 F+ FF
C
RT-PCR of Actn2 transcripts
1
5
6
7
8
9
ATG
Actn2:
AAV-Cre:
+/+ F/+ F/F F/+ F/F
wt–
ΔE2-6–
D
Rep 1
Rep 2
AGAGGAAGGATGACCC
Exon 1
Exon 7
E
Actn2:
AAV-Cre:
+/+ F/+ F/F F/+ F/F
WT
ΔE2-6
GAPDH
F
Actin Binding
Spectrin Repeats
CaM-like
ACTN2-WT
CH1 CH2 SR1 SR2 SR3 SR4 EF EF
ACTN2-ΔE2-6
aa42~204
G
AAV-ACTN2-WT
ITR cTNT ACTN2-WT GFP ITR
AAV-ACTN2- ΔE2-6
ITR cTNT ACTN2-ΔE2-6 GFP ITR
Full-dose AAV
wt mice
P1
P30
Analysis
H
AAV-ACTN2-WT
AAV-ACTN2- ΔE2-6
GFP
FM 4-64
GFP
FM 4-64
I
Length (μm)
(0.47)
Width (μm)
(0.97)
Length:Width
(0.57)
n=40 n=42
ACTN2-ΔE2-6-GFP
J
n=4 n=3 n=5
FS (%)
(0.85)
LVID;d (mm)
(0.11)
LVID;s (mm)
(0.30)
AAV: GFP ACTN2WT ACTN2ΔE2-6

Fig. S2. Generation of a conditional hypomorphic allele of *Actn2*. (A) Design of the *Actn2*^{F} allele. **(B)** Heart function of *Actn2*^{F} mice analyzed by echocardiography at 4-6 months of age. FS, fractional shortening. LVID;d and LVID;s, left ventricular internal diameter in diastole and systole, respectively. **(C-E)** P1 mice were treated with high dose AAV-Cre and ventricular RNA was analyzed by RT-PCR (C,D) and western blotting at P7. The predominant transcript after Cre recombination (C) was not the expected exon 2-4 deleted transcript but rather a transcript, named *Actn2ΔE2-6*, that resulted from ectopic splicing of exon 1 to exon 7 (D). ACTN2 western blot of control and mutant heart extracts using a C-terminal ACTN2 antibody (E) demonstrated expression of the internally deleted mutant protein. In the *Actn2*$^{F/F}$ mice, residual full length protein is likely due to about 25% of cardiomyocytes not being transduced by Cre and perdurance of the pre-recombination ACTN2 protein at this time point only 6 days after AAV treatment. Expression level of the truncated protein was much lower than full length ACTN2 in wild type mice. *Actn2ΔE2-6* transcript and protein were detected only when both the floxed allele and Cre were present (C,E), indicating that they resulted from Cre-mediated recombination and not from the unrecombined flox allele or from an effect of AAV-Cre alone. **(F)** Domain structure of wild-type and mutant ACTN2 proteins. The loss of exons 2-6 removes most of the actin binding domains of ACTN2. **(G)** Experimental design of AAV-mediated overexpression of wild-type and mutant ACTN2 tagged with GFP in cardiomyocytes. **(H)** In situ imaging of GFP and T-tubules in the heart. Arrows point to intercalated discs. ACTN2ΔE2-6 localized normally to Z-lines and had increased localization at intercalated disks, suggesting non-actin-binding dependent localization to proteins at the intercalated disk. Scale bar, 20 μm. **(I)** Morphometric measurement of isolated cardiomyocytes from hearts with mosaic overexpression of mutant ACTN2. Overexpressed ACTN2ΔE2-6 did not affect cardiomyocyte morphology. (**J**) ACTN2ΔE2-6 overexpression did not affect heart function. Wild-type mice were treated at P1 with the indicated AAV at a dose that transduces about 75% of cardiomyocytes. Echocardiography was performed at P30. Box plots symbols are described in the methods. Two-tailed student's *t*-test: Non-significant P-values are labeled in parentheses.

Figure S3

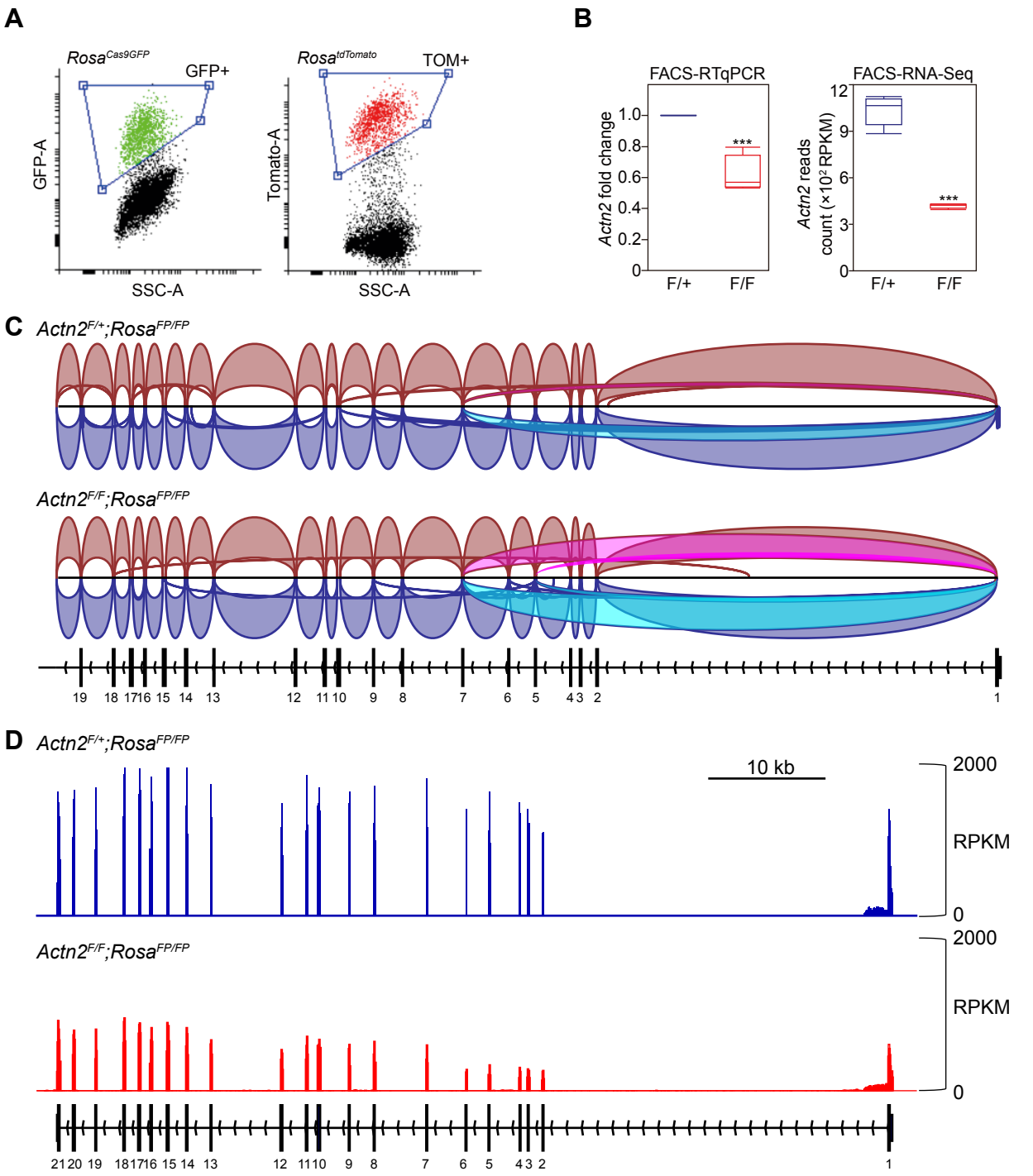

Fig. S3. FACS-RNA-seq of Actn2 mutant and control cardiomyocytes. We treated *Actn2*$^{F/F}$*;Rosa*$^{FP/FP}$ mice with mosaic ($3.6x10^8$ vg/g) dose of AAV-Cre at P1 and isolated cardiomyocytes at P14. **(A)** Representative FACS plots and gating to sort FP+ P14 cardiomyocytes. **(B)** Measurement of *Actn2* mRNA level in FACS-sorted FP+ cardiomyocytes by RT-qPCR (left) and RNA-seq (right) at P14. n=5 hearts per group. **(C)** Profiling *Actn2* splicing junctions by RNA-seq using integrative genome viewer. Each splice junction is represented by an arc from the beginning to the end of the junction. The thickness of the arc represents the reads counts. Junctions from the plus strand are colored red and extend above the center line. Junctions from the minus strand are blue and extend below the center line. The exon 1-5 and 1-7 junctions are highlighted in magenta and cyan. **(D)** The distribution of RNA-seq reads aligned to *Actn2* with a bin size of 50 bp. The heights of the bars represent normalized read counts.

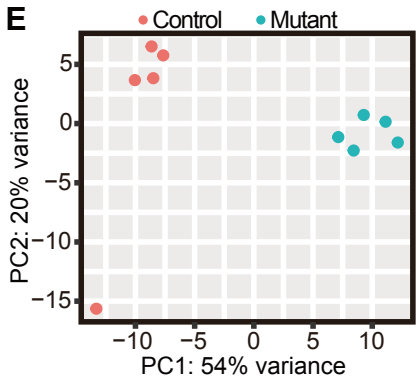

Fig. S3, con't. FACS-RNA-seq of Actn2 mutant and control cardiomyocytes.

(E) PCA plot of FACS-RNA-seq of Actn2 mutant and control cardiomyocytes. The individual replicates belonging to each group were well separated.

Figure S4

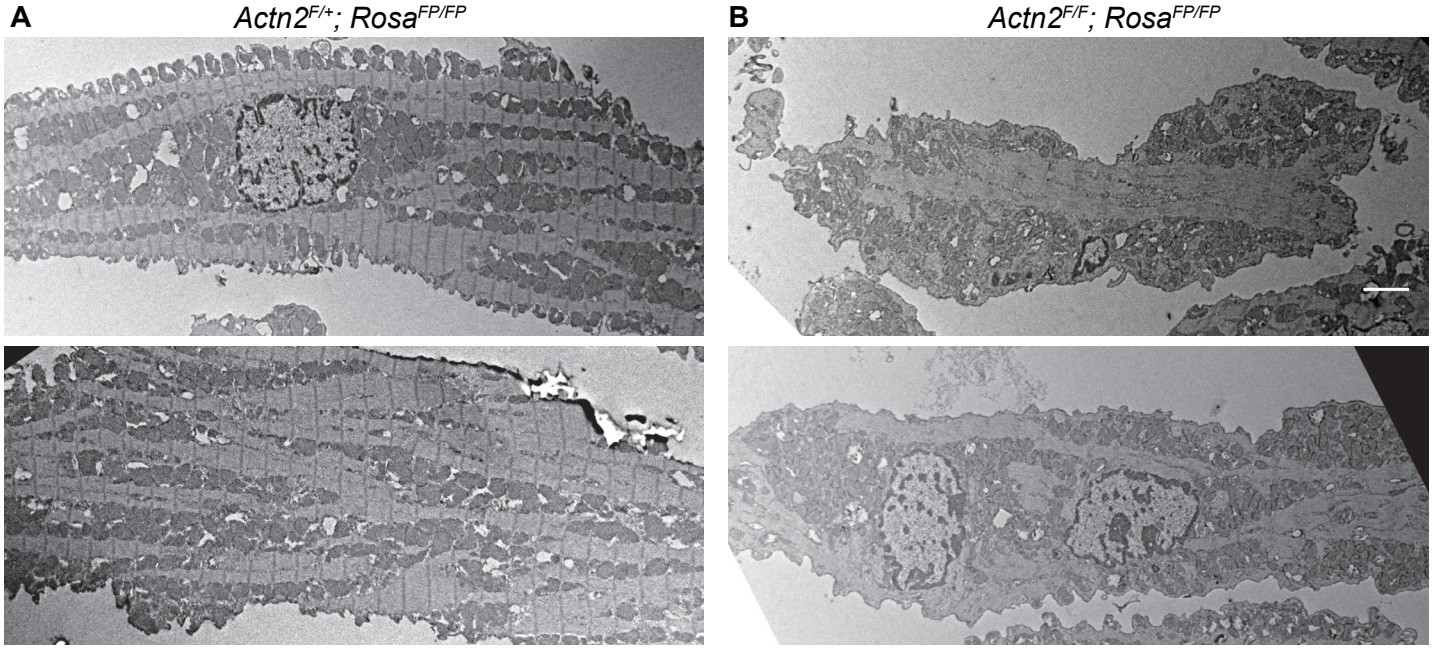

Fig. S4. Electron microscopy analysis. *Actn2$^{F/+}$; Rosa$^{FP/FP}$* **(A)** and *Actn2$^{F/F}$; Rosa$^{FP/FP}$* **(B)** mice were treated with AAV-Cre at P1. At P30, CMs were isolated from these mice, fixed by PFA, and subjected to FACS purification of FP+ cells. FP+ Control (A) and mutant CMs (B) were next processed and imaged by electron microscopy. Scale bar, 2 μm.

Figure S5

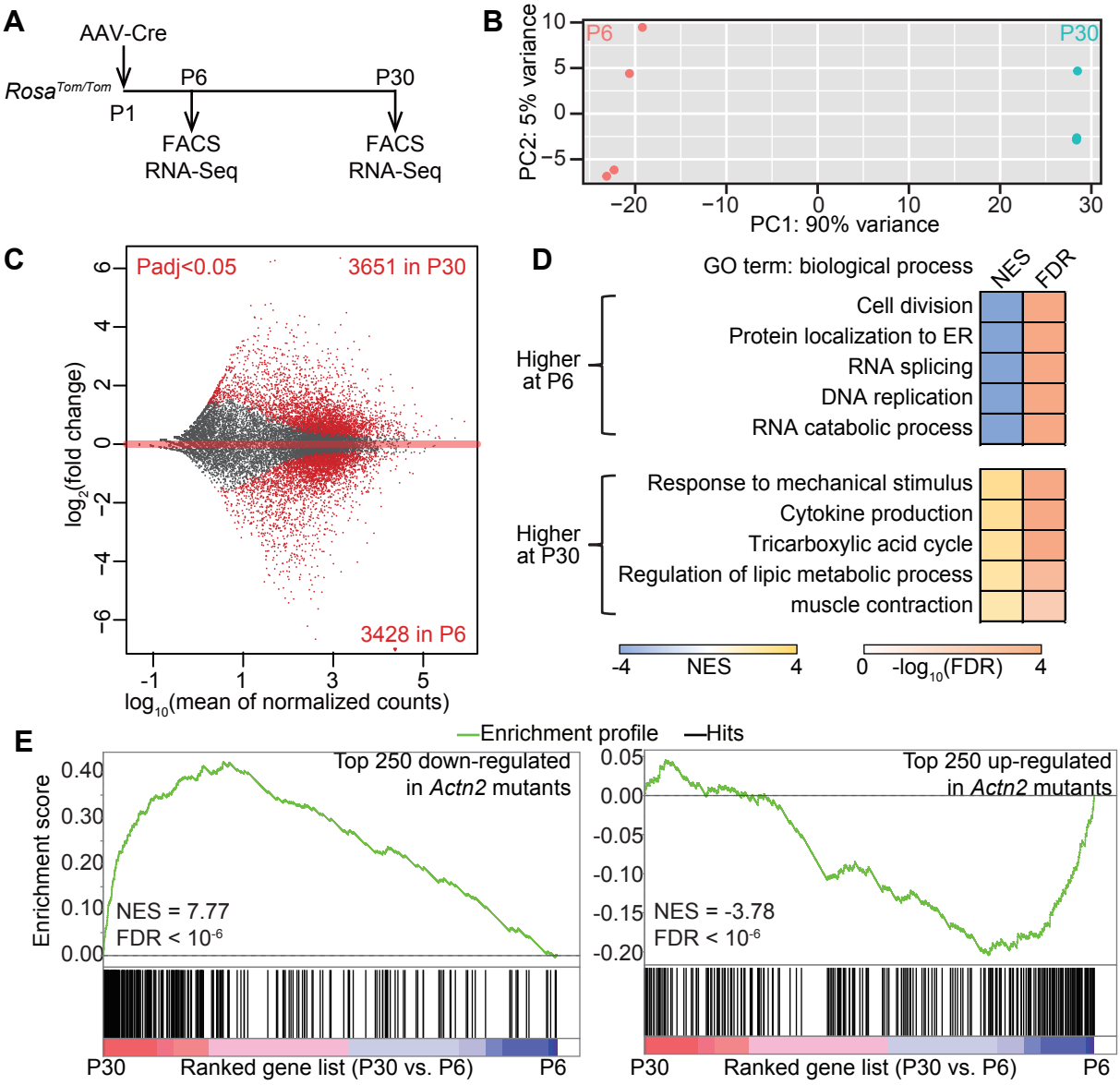

Fig. S5. Transcriptional maturation analysis using P6 and P30 CMs as reference. (A) Design of RNA-seq analysis of CMs at P6 and P30. **(B)** PCA of P6 and P30 CM transcriptomes. **(C)** MA plot of differential expression analysis between P6 and P30. **(D)** Representative GO terms that are enriched in P6 or P30 samples by GSEA. Negative and positive normalized enrichment score (NES) stands for enrichment at P6 or P30, respectively. **(E)** GSEA test of differentially expressed genes in *Actn2* mutant CMs using P6 vs. P30 data as reference.

Figure S6

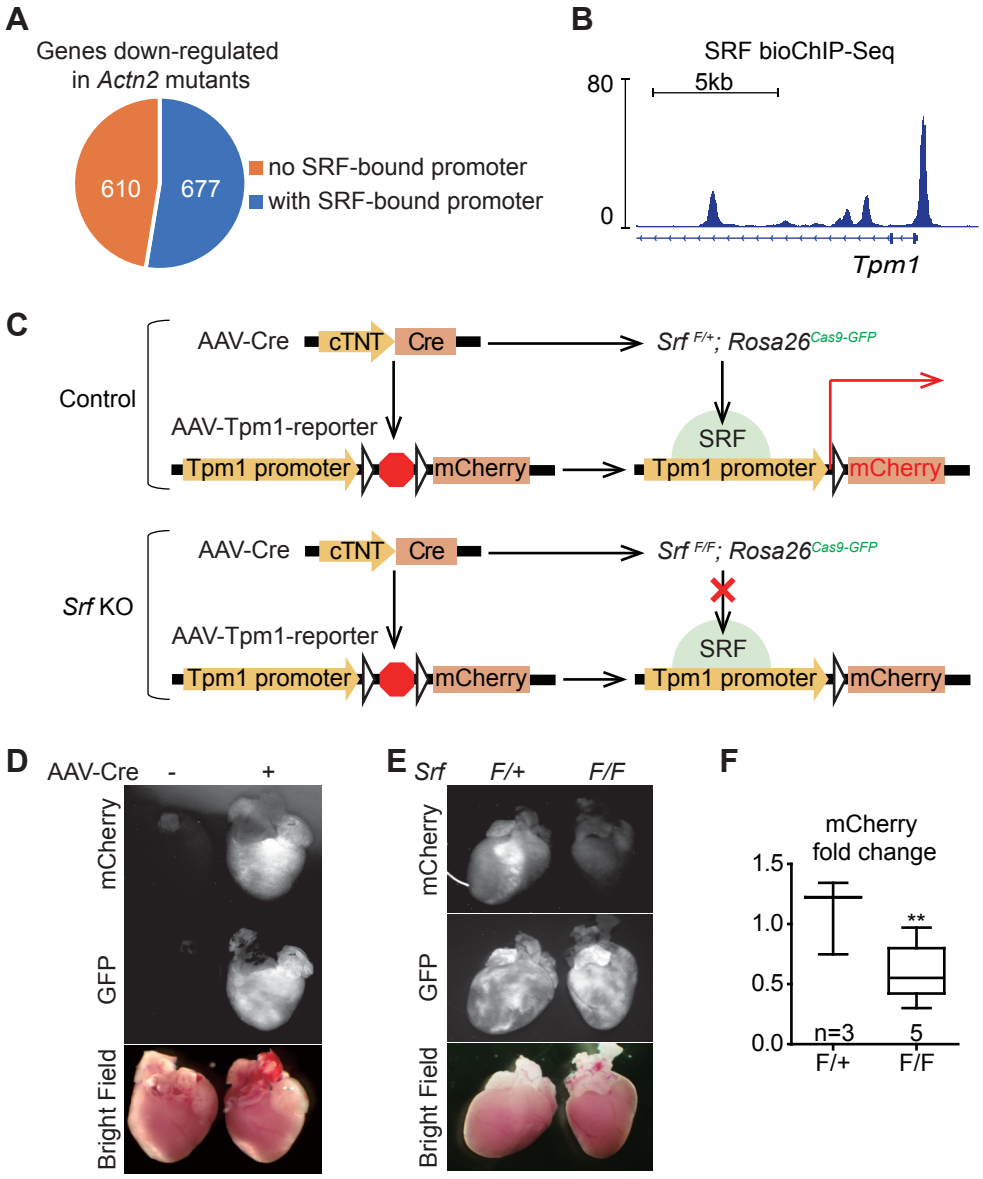

Fig. S6. *Tpm1* promoter depends on SRF for transcriptional activation. (A) The fraction of down-regulated genes in *Actn2* mutants with SRF-bound promoters (TSS±1kb). **(B)** SRF bioChIP-Seq results of P14 hearts on the promoter of *Tpm1* gene. **(C)** The design of a dual-AAV reporter assay to determine the impact of SRF on the *Tpm1* promoter *in vivo*. **(D)** Bright field and fluorescence images of $Rosa^{Cas9GFP}$ hearts that were transduced with $3.6x10^9$ vg/g AAV-Tpm1-LSL-mCherry reporter with or without $1.1x10^9$ vg/g AAV-Cre. **(E)** Bright field and fluorescence images of $Srf^{F/+}$;$Rosa^{Cas9GFP}$ or $Srf^{F/F}$;$Rosa^{Cas9GFP}$ hearts that were co-transduced with AAV-Tpm1-LSL-mCherry reporter and AAV-Cre. **(F)** RTqPCR analysis of mCherry reporter expression in $Srf^{F/+}$ vs. $Srf^{F/F}$ ventricles, normalized to *Gapdh* expression in the same tissue. Student's *t*-test: **p<0.01.

Figure S7

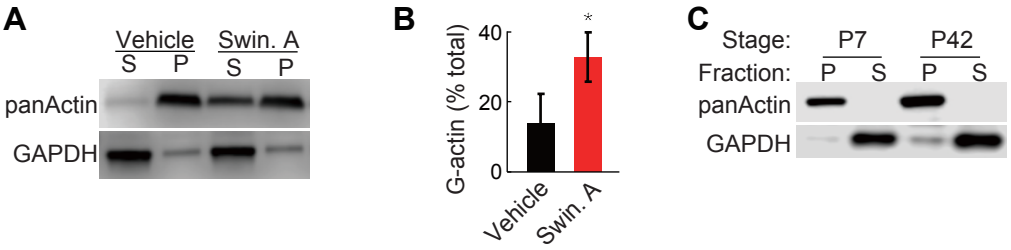

Fig. S7. Assessment of actin polymerization by the actin pelleting assay. (A) Western blot showing increased actin in supernatant (S) compared to pellet (P) upon 5 μM swinholide A treatment of WT heart lysate. **(B)** Densitometric quantification of relative G-actin (supernatant) and F-actin (pellet) in WT heart lysates by actin pelleting. n=3; error bar, SD. Student's t-test: *, $p<0.05$. **(C)** Actin pelleting analysis of P7 and P42 WT heart lysates.

Figure S8

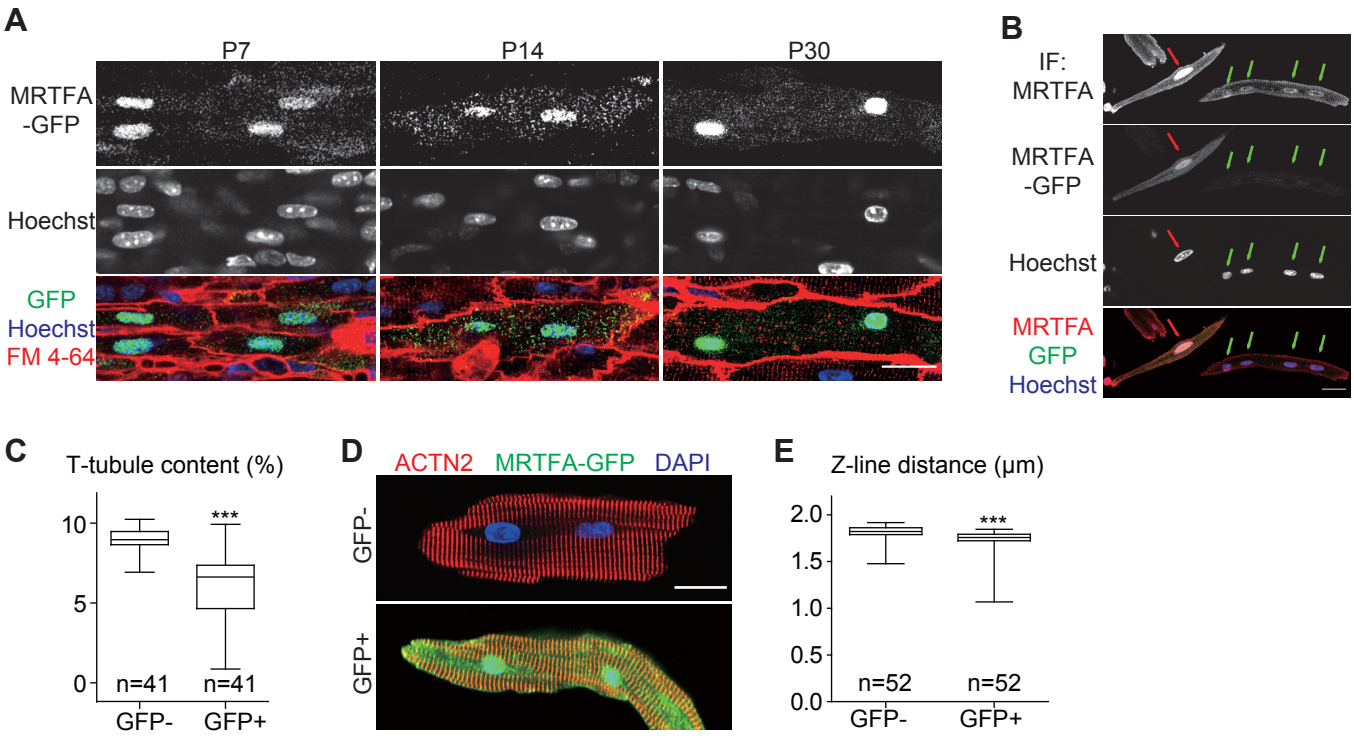

Fig. S8. MRTFA subcellular localization and overexpression. (A) *In situ* imaging reveals MRTFA-GFP localization. Wild-type hearts transduced with AAV-MRTFA-GFP were perfused with Hoeschst and FM 4-64 dyes, which label nuclei and sarcolemma, respectively. The hearts were then optically sectioned using a confocal microscope. **(B)** Immunolocalization of endogenous and overexpressed MRTFA. AAV-MRTFA-GFP transduced hearts were dissociated and CMs were immunostained with MRTFA antibody. Untransduced CMs (GFP-) showed weak MRTFA immunoreactivity in their nuclei (green arrows). Transduced CMs (GFP+) showed stronger MRTFA predominantly in the nucleus. (red arrow). **(C)** Quantification of T-tubule content in hearts transduced with AAV-MRTFA-GFP. **(D)** Immunofluorescence analysis of ACTN2 in AAV-MRTFA-GFP transduced (GFP+) and untransduced (GFP-) cardiomyocytes from the same heart. **(E)** Quantification of sarcomere Z-line distance in cardiomyocytes that were untransduced (GFP-) or transduced (GFP+) with AAV-MRTFA-GFP. In all images, scale bar represents 20 μm.

Figure S9

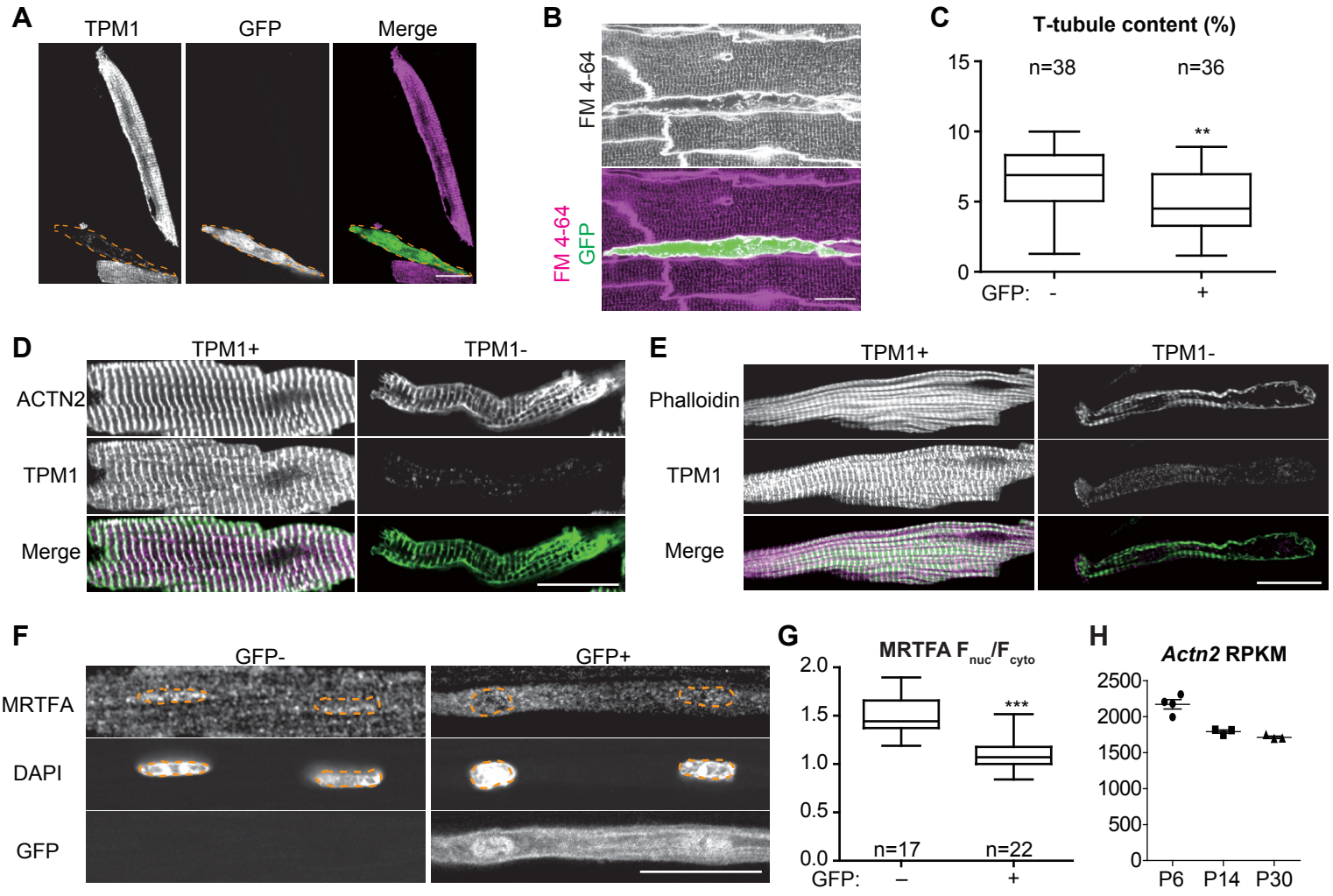

Fig. S9. TPM1 depletion perturbs cardiomyocyte morphological maturation and MRTFA nuclear localization. (A) Immunofluorescence of TPM1 in cardiomyocytes that were isolated from hearts treated by *Tpm1* CASAAV. A TPM1-depleted cell is delineated in orange. **(B)** *In situ* T-tubule imaging of a heart treated by *Tpm1* CASAAV. **(C)** AutoTT-based quantification of T-tubule content in CASAAV treated cardiomyocytes. **(D-F)** Immunofluorescence of ACTN2 **(D)**, Phalloidin **(E)** and MRTFA **(F)** in TPM1-depleted cardiomyocytes. In all images, scale bars represent 20 μm. **(G)** Quantification of nuclear vs. cytoplasmic MRTFA by immunofluorescence intensity measurement. **(H)** *Actn2* RNA-seq normalized reads counts at P6, P14 and P30. Student's t-test: **p<0.01, ***p<0.001.

Figure S10

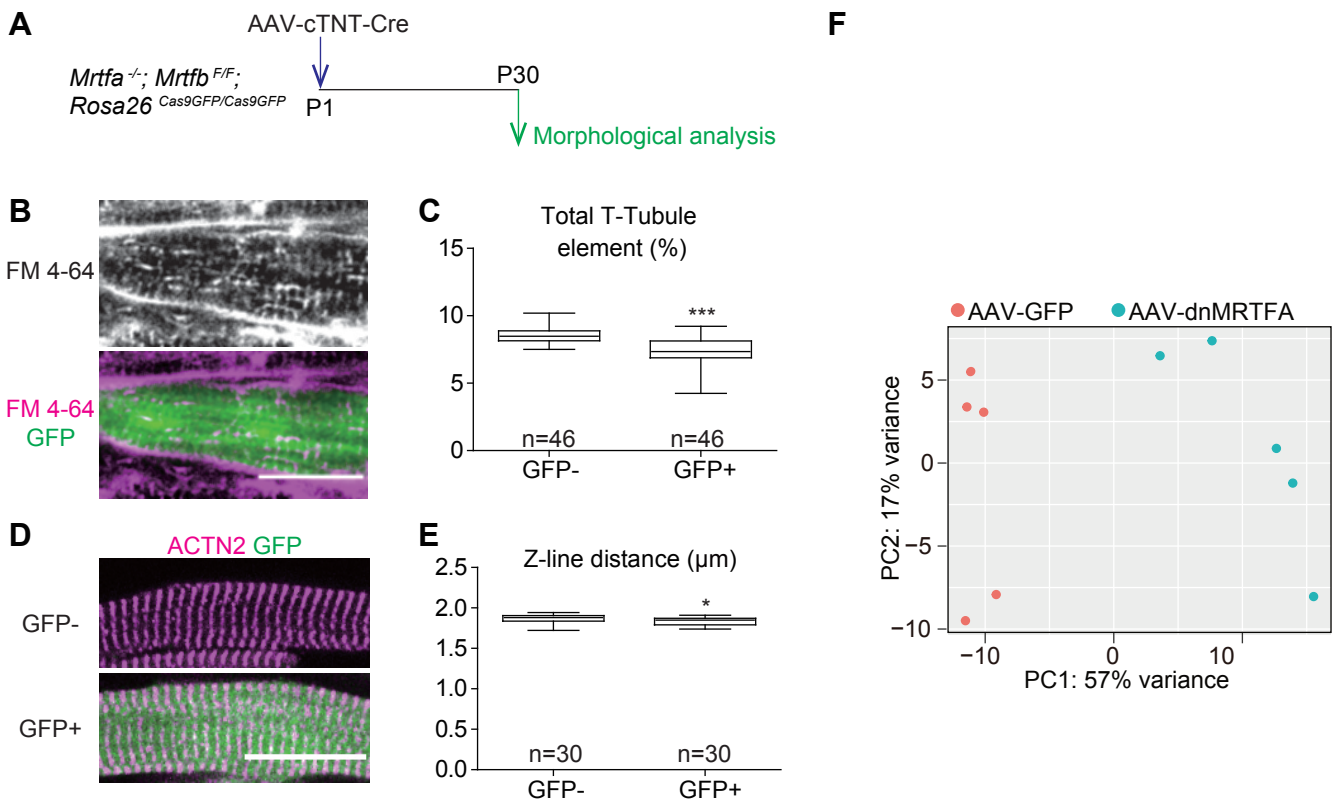

Fig. S10. MRTFA/B are required for cardiomyocyte maturation. (A) Experimental design to generate MRTFA/B mosaic double knockout in cardiomyocytes *in vivo*. **(B)** *In situ* T-tubule imaging of MRTFA/B mosaic double knockout hearts. **(C)** AutoTT quantification of T-tubule content. **(D)** ACTN2 immunofluorescence in cardiomyocytes that were isolated from MRTFA/B mosaic double knockout hearts. **(E)** Quantification of sarcomere Z-line distance. **(F)** RNA-seq of cardiomyocytes expressing dnMRTFA. P1 pups were treated with AAV expressing dnMRTFA or GFP. At P14, transduced cardiomyocytes were purified by FACS. Gene expression was analyzed by PCA. In **(C)** and **(E)**, Student's t-test:*p<0.05, ***p<0.001. Scale bar = 20 μm.

Supplementary Table 1. Summary of RNA-seq data in this study

Experiment	Group	Genotype	AAV	Replicates	Uniquely Aligned reads to mm10 by STAR	Reference
Actn2 mutation	control	Actn2-F/+	AAV-Cre	1	25237696	This study
Actn2 mutation	control	Actn2-F/+	AAV-Cre	2	8639028	This study
Actn2 mutation	control	Actn2-F/+	AAV-Cre	3	8086656	This study
Actn2 mutation	control	Actn2-F/+	AAV-Cre	4	8815555	This study
Actn2 mutation	control	Actn2-F/+	AAV-Cre	5	10309615	This study
Actn2 mutation	Actn2 mutant	Actn2-F/F	AAV-Cre	1	9764430	This study
Actn2 mutation	Actn2 mutant	Actn2-F/F	AAV-Cre	2	12707923	This study
Actn2 mutation	Actn2 mutant	Actn2-F/F	AAV-Cre	3	9993533	This study
Actn2 mutation	Actn2 mutant	Actn2-F/F	AAV-Cre	4	9265270	This study
Actn2 mutation	Actn2 mutant	Actn2-F/F	AAV-Cre	5	16892340	This study
dnMRTF treatment	control	wildtype	AAV-GFP	1	15226384	This study
dnMRTF treatment	control	wildtype	AAV-GFP	2	8668918	This study
dnMRTF treatment	control	wildtype	AAV-GFP	3	9028580	This study
dnMRTF treatment	control	wildtype	AAV-GFP	4	17294020	This study
dnMRTF treatment	control	wildtype	AAV-GFP	5	14999634	This study
dnMRTF treatment	dnMRTF	wildtype	AAV-dnMRTF-GFP	1	9947030	This study
dnMRTF treatment	dnMRTF	wildtype	AAV-dnMRTF-GFP	2	10415225	This study
dnMRTF treatment	dnMRTF	wildtype	AAV-dnMRTF-GFP	3	8501445	This study
dnMRTF treatment	dnMRTF	wildtype	AAV-dnMRTF-GFP	4	16848098	This study
dnMRTF treatment	dnMRTF	wildtype	AAV-dnMRTF-GFP	5	14906078	This study
SRF KO	control	Srf-F/+	AAV-Cre	1	20752681	2
SRF KO	control	Srf-F/+	AAV-Cre	2	21204212	2
SRF KO	control	Srf-F/+	AAV-Cre	3	16829857	2
SRF KO	SRFKO	Srf-F/F	AAV-Cre	1	16733251	2
SRF KO	SRFKO	Srf-F/F	AAV-Cre	2	18215520	2
SRF KO	SRFKO	Srf-F/F	AAV-Cre	3	16689997	2
P6_vs_P30	P6	Rosa-FP	AAV-Cre	1	10594932	This study
P6_vs_P30	P6	Rosa-FP	AAV-Cre	2	27506075	This study
P6_vs_P30	P6	Rosa-FP	AAV-Cre	3	51427646	This study
P6_vs_P30	P6	Rosa-FP	AAV-Cre	4	11515303	This study
P6_vs_P30	P30	Rosa-FP	AAV-Cre	1	16518023	This study
P6_vs_P30	P30	Rosa-FP	AAV-Cre	2	17058353	This study
P6_vs_P30	P30	Rosa-FP	AAV-Cre	3	20525128	This study

Supplementary Table 2. Antibodies and Dyes

Antibodies					
Antigen	**Source of Species**	**Vendor/ Source**	**Cat. #**	**Working concentration**	**Application**
ACTN2	Rabbit	Novus Biologicals	NBP1-90376	1:200 (IF), 1:2000 (WB)	IF, WB
GAPDH	Rabbit	Life Technologies	PA116777	3.5138889	WB
MRTF	Rabbit	Gift from Guido Posern Lab	NA	1:200 (IF), 1:2000 (WB)	IF, WB
ACTC1	Mouse	Millipore	MABT823	1.7777778	WB
panActin	Rabbit	Cytoskeleton	AAN01	3.5138889	WB
LMNB1	Rabbit	Abcam	ab16048	1.4305556	WB
FLAG	Mouse	Sigma Aldrich	F1804	1.4305556	WB
HA	Rabbit	Abcam	ab9110	1.4305556	WB

Dye				
Name	**Vendor**	**Cat. #**	**Working concentration**	**Application**
FM 4-64	Invitrogen	T-3166	2ug/ml	In situ imaging
TMRM	Invitrogen	T668	200nM	In situ imaging
WGA-633	Invitrogen	W32466	5µg/ml	IF
Hoechst	Invitrogen	H1399	4ug/ml	In situ imaging
Phalloidin	Cytoskeleton	PHDH1-A	14nM	IF
DAPI	Invitrogen	D3571	500nM	IF